

The origin of life from primordial planets

Carl H. Gibson¹, Rudolph E. Schild² and N. Chandra Wickramasinghe³

¹University of California San Diego, La Jolla, CA 92093-0411, USA

e-mail: cgibson@ucsd.edu

²Center for Astrophysics, 60 Garden Street, Cambridge, MA 02138, USA

e-mail: rschild@cfa.harvard.edu

³Cardiff Centre for Astrobiology, 24 Llwynypia Road, Lisvane, Cardiff CF14 0SY, UK

e-mail: NCWick@gmail.com

Abstract: The origin of life and the origin of the Universe are among the most important problems of science and they might be inextricably linked. Hydro-gravitational-dynamics cosmology predicts hydrogen–helium gas planets in clumps as the dark matter of galaxies, with millions of planets per star. This unexpected prediction is supported by quasar microlensing of a galaxy and a flood of new data from space telescopes. Supernovae from stellar over-accretion of planets produce the chemicals (C, N, O, P, etc.) and abundant liquid-water domains required for first life and the means for wide scattering of life prototypes. Life originated following the plasma-to-gas transition between 2 and 20 Myr after the big bang, while planetary core oceans were between critical and freezing temperatures, and interchanges of material between planets constituted essentially a cosmological primordial soup. Images from optical, radio and infrared space telescopes suggest life on Earth was neither first nor inevitable.

Received 15 June 2010, accepted 9 August 2010, first published online 22 September 2010

Key words: Cosmology, astrobiology, primordial planets, dark matter.

Introduction

After a long and careful study of cosmic panspermia with one of the authors (NCW), Fred Hoyle suggested in 1980 that ‘... the cosmic quality of microbiology will seem as obvious to future generations as the Sun being the centre of the Solar System seems obvious to the present generation ...’ (Wickramasinghe 2005). Panspermia is the ancient idea that life seeds are distributed everywhere in the cosmos (Anaxoragas, 500 BC). Panspermia theories (Hoyle & Wickramasinghe 1977, 1982, 2000) and the field of astrobiology have been greatly hampered by the lack of feasible mechanisms for the large-scale transmission of microbiological information between planets within the standard (Λ CDMHC) cosmological model where planets are produced by stars and stars are produced by gas. The collision time between planets of different stars of a galaxy by the cold-dark-matter (CDM) hierarchical clustering (HC) model with dark energy (Λ) is roughly a billion times the age of the present Universe. Because a key result of hydro-gravitational-dynamics (HGD) is that the dark matter of galaxies is dense clumps of ancient planets, each of which is a potential host for life, this first-order argument against astrobiology and cosmological panspermia (Wickramasinghe *et al.* 2004; Wickramasinghe & Napier 2008; Wickramasinghe 2010) is removed.

The Λ CDMHC (the standard cosmological model) shows that it is highly improbable that life could be widely transferred in the cosmos, and impossible for life to begin. The

extreme complexity of the simplest living microorganism suggests spontaneous creation (abiogenesis on any local non-cosmological scale) is impossible without templates. HGD (Gibson 1996; Nieuwenhuizen *et al.* 2009) provide the fluid mechanical processes and the large time periods that Λ CDMHC lacks for life on Earth to exist in its present state. Galaxy microlensing of a quasar discussed by one the authors (RES) reveals planetary mass twinkling frequencies that support the conclusion that planets constitute the missing mass of galaxies (Schild 1996). HGD cosmology predicts that the optimum time for first life to appear is soon after plasma became gas 13.7 Gyr ago (Gibson & Wickramasinghe 2010). HGD suggests that the early seeds of life should be rapidly and widely scattered on cosmic scales and collected gravitationally by the trillion planets expected within each clump. Evaporated atmospheres of the frozen gas planets are photo-ionized to detectably large scales in planetary nebula, such as Helix. An Oort-type cloud of long-period comets is revealed in Fig. 1 to actually be proto-comet planets at the boundary of a cavity in the proto-globular star cluster (PGC) clump of dark matter planets of size reflecting the large primordial mass density of the planets and the mass of the star or binary star formed in the centre that have converted the H–He comets to a rapidly spinning carbon white dwarf.

Evidence from new telescopes, and improved old telescopes, show the standard cosmological model Λ CDMHC requires major modification to include the effects of modern fluid mechanics (Gibson 2009a, b). Including viscosity, diffusivity and stratified turbulent transport processes requires a

Spitzer infrared view of nearby Helix planetary nebula

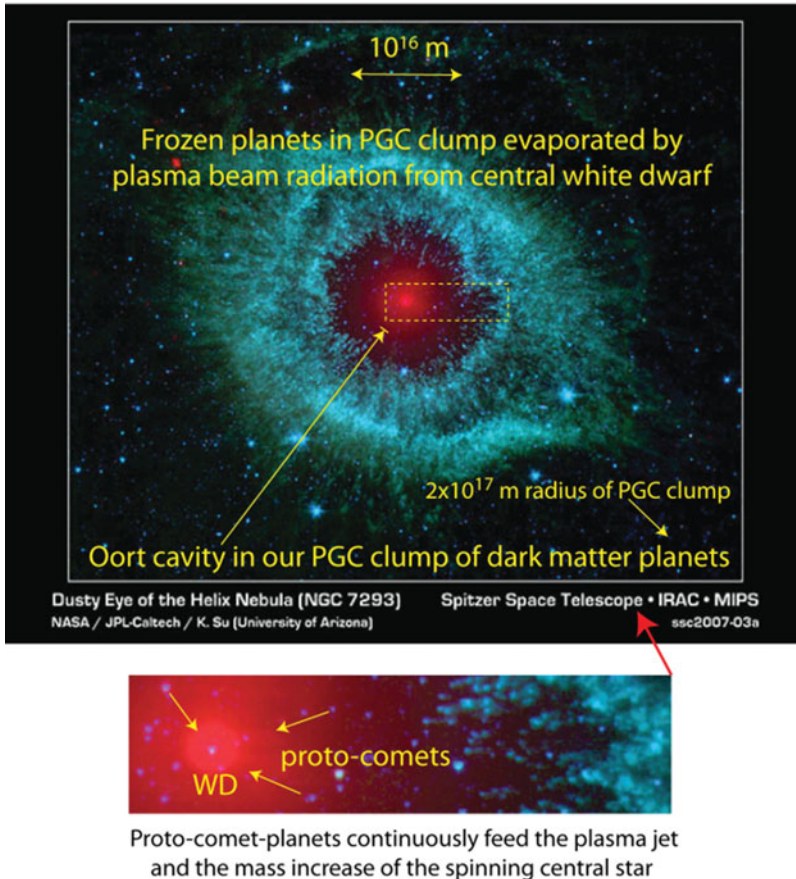


Fig. 1. Spitzer space telescope infrared view of Helix PNe at 6.7×10^{18} m. The central white dwarf converts the hydrogen–helium frozen gas of proto-comets shown in the dashed box (bottom insert) to carbon of the shrinking star, and to a plasma jet that partially evaporates the ambient dark matter planets of the PGC clump of dark-matter planets. The red dust cloud about the white dwarf is presumably left by the accreted proto-comets as they evaporate near the star, feeding its growth toward instability.

new cosmology started by big-bang turbulence and its fossils. From HGD, CDM does not exist and neither does the standard (non-turbulent, inviscid) dark energy (Λ) invented by Einstein to produce a static universe by anti-gravity. From HGD, the dark matter of galaxies is primordial planets in clumps that dominate the mass of the interstellar medium and the formation, evolution and death of stars. The mass of non-baryonic dark matter (NBDM) appears to be ~ 30 times more, in the form of primordial neutrinos, and is weakly collisional and very hot, diffused away from 10^{22} m galaxy halo scales to 10^{23} m galaxy cluster halo scales and larger. Such matter is dynamically irrelevant to galaxy and star evolution.

According to our favoured, and in our view correct, cosmological model, HGD, planets form all the stars, as well as their comets, in a sequence of powerful binary mergers that continually recycle life seeds, fertilizer and ecosystems. This also, incidentally, explains why most stars are binary. Radio telescope signals from these 10^5 -times-a-day events have recently been detected (Ofek *et al.* 2010) and identified as either an inexplicable galactic population of neutron stars or nearby exotic interstellar explosions without optical or

infrared counterparts. The gravitational explosive power of a 10-Jupiter merger occurring in a three-month period corresponds to that of a million suns, and can account for the radio telescope signals observed, and also produce the recycling of materials of the larger and smaller objects produced. Together the planets, moons and comets of a PGC collect and redistribute life-giving stardust and life prototypes throughout the galaxy and galaxy clusters.

Runaway accretion of planet proto-comets leads to supernova deaths of stars that expel thousands of planets throughout the primordial planet clumps along with stardust fertilizer, water, carbon and life infections and organic waste products of other planets. According to HGD, life is common in the cosmos and has existed throughout all space at galaxy and galaxy-cluster scales since soon after the gas epoch began. The ability of living organisms to efficiently convert most of the carbon of a planet to complex organic compounds that absorb and reradiate light differently than abiological carbon compounds may explain the ultra-luminous infrared galaxy (ULIRG) phenomenon (for example, Veilleux *et al.* 2009), rather than dusty quasar mergers. A new class of blue galaxies detected to redshift

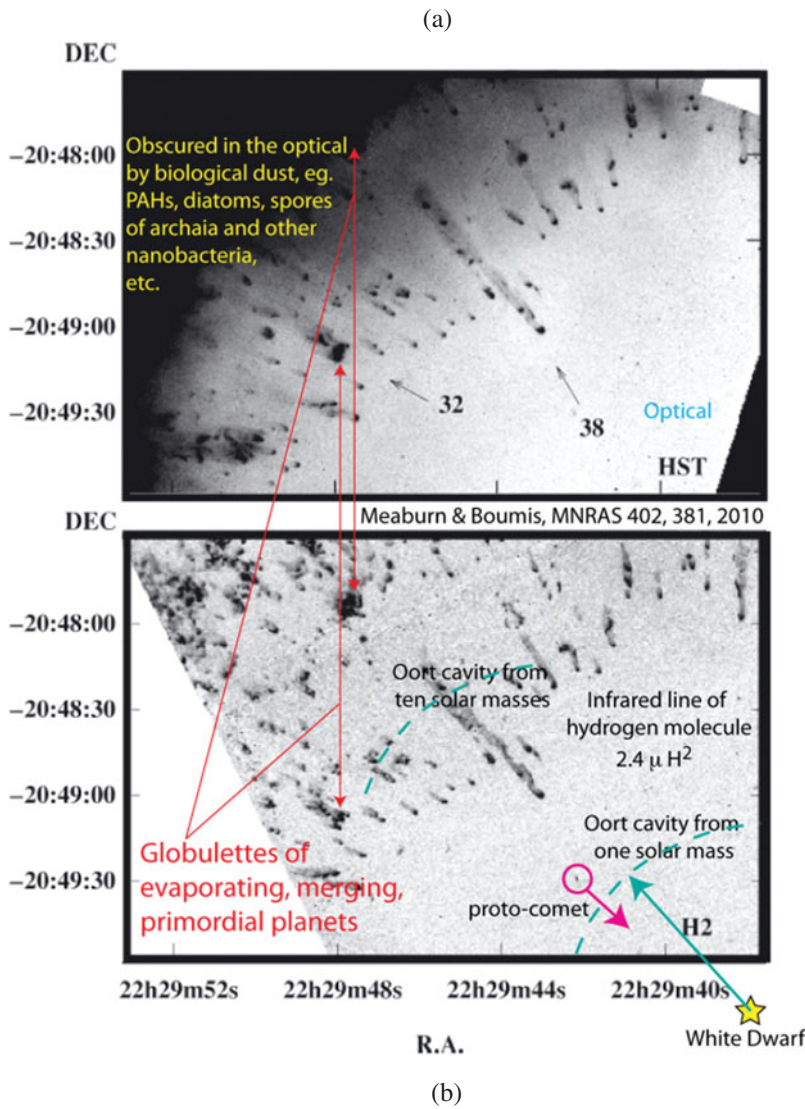


Fig. 2. Images from the HST of the Helix planetary nebula in the optical (a) and 2.4 μ H² infrared (b), from Meaburn & Bourmis (2010). Dust from evaporating frozen gas planets at the Oort cavity boundary (b) obscures clumps of merging planets (globulettes, Gahm *et al.* 2007) in the optical (a). Most hydrogen wakes point towards the central white dwarf star ((b), right-hand side). The planet numbered 38 (a) has a 2.4×10^{14} m diameter atmosphere with mass over 10^{26} kg, suggesting a massive (~Jupiter) evaporating frozen planet within.

$z > 10$ appears to be dust free, possibly because life and its wastes had not yet had time to develop (Bouwens *et al.* 2009; Gibson 2010, Fig. 2).

The plan of this paper is to first discuss the formation of clumps of primordial planets at the plasma-to-gas transition in the very early Universe, since this is where the first life forms probably appeared. The following section compares non-standard (correct) HGD and the standard LCDMHC cosmologies in relation to mechanisms for the origin of life and panspermia. Finally, discussion and conclusion sections are presented.

The formation of primordial planets in clumps

Observations support a big-bang event (Peebles *et al.* 2009), where the spectral lines of distant objects are red shifted by a stretching of space in an expanding universe according to

Einstein’s equations of general relativity (Peacock 2000). General agreement exists (Weinberg 2008) that the big-bang event was hot and produced a primordial plasma of protons, alpha particles and electrons with mass energy dominated by mass at about 10^{11} seconds (3000 years) after the big-bang event and the plasma-to-gas transition at 10^{13} s (300 000 years). Unfortunately, strong fluid mechanical simplifications necessary in the early days of cosmology have been continued to this day. It has been assumed that the fluids of the early Universe are frictionless, irrotational, linear and ideal. They are not. The relevance of fluid mechanics to astrobiology arises from the HGD prediction that the dark matter of galaxies is frozen H-He planets in clumps with appropriate admixtures of biogenic elements (Gibson & Wickramasinghe 2010). How does this happen?

Viscosity is neglected in the standard cosmology model based on the Jeans 1902 acoustical criterion for gravitational

structure formation in a gas (Jeans 1902). By this criterion, gravitational structure formation begins when the Jeans length scale $L_J = V_S/(\rho G)^{1/2}$ becomes smaller than the horizon scale, or the scale of causal connection, $L_H = ct$, where V_S is the speed of sound, ρ is the density, G is Newton's gravitational constant, c is the speed of light and t is the time. Jeans used the inviscid Euler equations, linear perturbation theory and neglected diffusivity effects that turn out to be crucial. These strong assumptions reduce the momentum conservation equations to a linear acoustic form and the Jeans criterion for structure formation. No gravitational structure can form during the plasma epoch, $10^{11} \text{ s} < t < 10^{13} \text{ s}$, because the Jeans length scale, $L_J = V_S/(\rho G)^{1/2}$, is less than the scale of causal connection, $L_H = ct$, throughout this time period, where c is the speed of light and t is the time. The reason this is true is that the relevant density is that of the baryons that retain density fluctuations from big-bang turbulence. The total density of the Universe is dominated by weakly collisional non-baryons (neutrinos), which are so strongly diffusive that all non-baryonic density fluctuations are smoothed away. The baryonic gravitational free fall time $(\rho G)^{-1/2}$ is ~ 2.7 times larger than the critical value, causing failure of the Jeans criterion and the invention of cold dark matter.

Viscous forces prevent structure formation in the plasma epoch, while $L_H < L_{SV} = (\gamma v / \rho G)^{1/2}$, where γ is the rate of strain, v is the kinematic viscosity and L_{SV} is the Schwarz viscous-gravitational length scale (Gibson 1996). The kinematic viscosity v of the plasma is enormous (Gibson 2000), permitting proto-supercluster (PSC) void formation to begin when $L_H = L_{SV}$ at $t = 10^{12} \text{ s}$. Photon viscosity ceases when the cooling plasma turns to gas at $t = 10^{13} \text{ s}$. Because the gas viscosity is 10^{13} smaller, the fragmentation mass decreases by a factor of $(10^{13})^{3/2}$; that is, from galaxy mass 10^{43} kg to Earth mass $\sim 10^{24} \text{ kg}$. An additional gravitational instability occurs at L_J due to a mismatch between heat transfer at the speed of light and pressure transfer at the speed of sound, so fragmentation at the plasma-gas phase change produced 10^{36} kg Jeans-mass clumps of Earth-mass planets. These are PGC clumps of primordial-fog-particle (PFP) planets (Gibson 1996).

The PGC density is the baryonic density at the 10^{12} s time of first structure $\rho_0 = 4 \times 10^{-17} \text{ kg m}^{-3}$ that is observed in old globular star clusters (OGCs) of all galaxies. Stars form within such PGC clumps by mergers of the planets. If stars do not form but the planets freeze as the expanding Universe cools, these clumps of frozen planets become the dark matter of galaxies and most of the mass of the interstellar medium. Objects of mass M leave an $(M/\rho_0)^{1/3}$ size empty Oort cavity of missing planets in a PGC clump, which grows as the central object grows, to a $3 \times 10^{15} \text{ m}$ size for one star. Proto-comets from the cavity boundary continuously feed the growth of the inner star and will eventually cause its death when its mass exceeds the Chandrasekhar limit of 1.44 solar masses when the star is a white dwarf. As evidence, consider the Spitzer space telescope infrared image of the Helix planetary nebula shown in Fig. 1. The central star of Helix is a rapidly spinning white dwarf that converts the accreted planet

'proto-comets' to gas. Part of the gas is converted by the star to more carbon, and part is emitted at the poles as a plasma jet that evaporates any planets it encounters. The photo-ionized atmospheres and their wakes are large enough to be visible, between 10^{13} and 10^{14} m in diameter (an astronomical unit is $\sim 10^{11} \text{ m}$, the size of the Solar System).

All of the planets shown in Fig. 1, as well as the proto-comets and moons of planets forming orbital systems deep within the Oort cavity, are potential hosts for life.

Figure 2 shows optical and infrared evidence of primordial planets and their (presumably) biologically generated dust in PNe Helix (Matsuura *et al.* 2009; Meaburn & Boumis 2010). The differences in opacity between radio, infrared and optical frequencies offers a powerful tool for exploring the probabilities of life formation. Evidence from new infrared space telescopes Spitzer, Planck and Herschel shows that optically opaque dust is not always formed where planets exist on PGC scales. If dust clouds containing such polycyclic aromatic hydrocarbon (PAH: oils) and anthracite (coal) spectral signatures have a biological origin, then abiological processes must be extremely improbable on average planets like Earth, considering the variety of panspermic mechanisms and long time periods offered by HGD cosmology.

Figure 2(a) is an optical image (Meaburn & Boumis 2010) of planetary nebula Helix from the Hubble space telescope (HST), showing evaporating planets at the Oort-cavity boundary surrounding the central white dwarf compared to $2.4 \mu\text{m H}^2$ line images unobscured by dust (Matsuura *et al.* 2009).

Figure 3(a(i)) is the unobscured infrared Subaru telescope image (Matsuura *et al.* 2009) showing proto-cometary planets, detectable from their relatively small 10^{12} – 10^{13} m^2 atmospheres, on their way to feed the central star, but invisible (Fig. 3(a(ii))) in the dust-obscured HST optical image. Larger diameter (10^{13} – 10^{14} m) radiation-heated planet atmospheres appear in both Fig. 3(a) images beyond the edge of the Oort cavity. Correspondingly larger radiation pressures accelerate such planets radially outward, expelling the more dusty planets surrounding the central star into the interior of the PGC planet clump along with whatever biological templates, organisms and wastes the planets contain.

Sizes of sphere radii containing one, ten and a million (PGC boundary) solar masses from the expression $(M/\rho_0)^{1/3}$ are shown in Fig. 3(a). A proto-type PAH molecule is shown in Fig. 3(a(ii)). The structure is characteristic of carbohydrate oil used for food by terrestrial organisms, and is suggested as the signature of biological waste products expelled in differing amounts by radiation-evaporating biologically inhabited gas planets of the Helix planetary nebula.

Arguments for non-biologically generated PAHs in interstellar clouds are insecure, particularly so because of the requirement that over 20 % of interstellar carbon has to be tied up in this form. Biological aromatic molecules can be shown to produce the infrared bands that are astronomically without *ad hoc* assumptions about the nature and ionization states of inorganic PAHs (Gibson & Wickramasinghe 2010). Moreover, the extended red emission (ERE) observed in

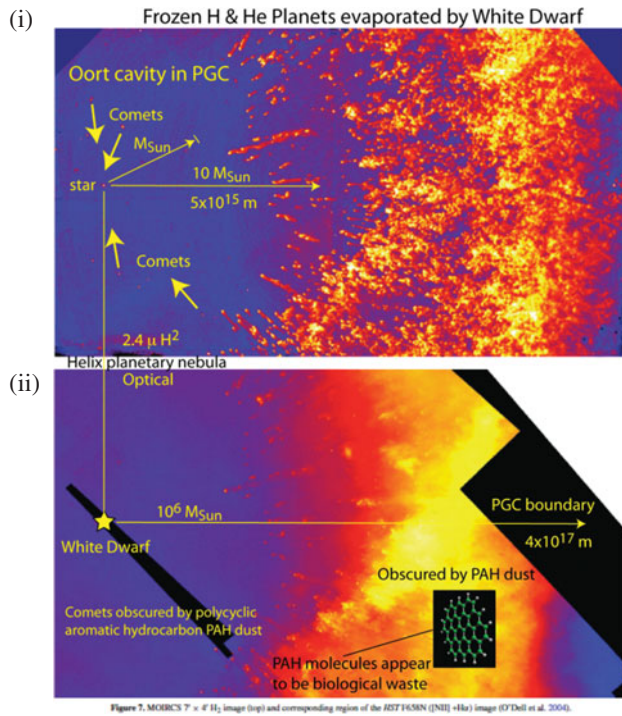
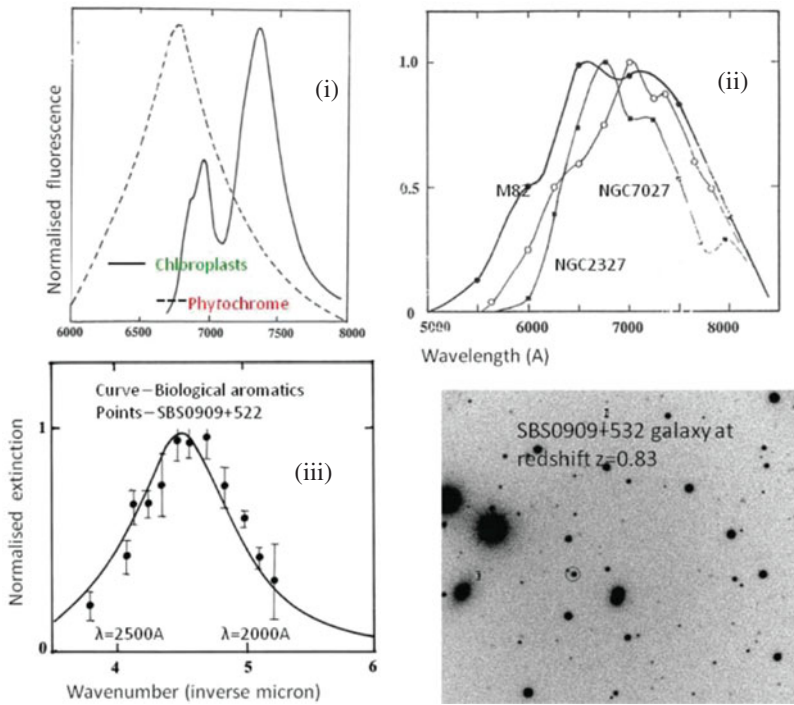


Figure 7. MORCS 7 × 4 H₂ image (top) and corresponding region of the HST F555W (NI) +H_α image (Y Del et al. 2004).

(a)



(b)

Fig. 3. (a) Images from the Subaru telescope of Helix planets and comets in the $2.4 \mu \text{H}^2$ frequency band (i) compared to the HST optical image (ii) in at optical frequencies (Matsuura *et al.* 2009, Fig. 7). Proto-comet planets (i) fall towards the central white dwarf because their biological dust content, atmosphere size and radial radiation pressures are smaller. (b) (i) Shows normalized fluorescence spectra of chloroplasts and phytochrome, which are complex biological PAHs. (ii) ERE first discovered by Witt & Schild (1988) and observed for many galactic and extragalactic sources. (iii) Normalized extinction excess for the gravitationally lensed galaxy SBS0909 + 522 (at redshift $z=0.83$) observed by Motta *et al.* (2002) compared with 115 biological aromatic compounds (see Hoyle & Wickramasinghe 2000). The comparison in (iii) shows that biological waste products were evident in dust when the Universe was half its present size.

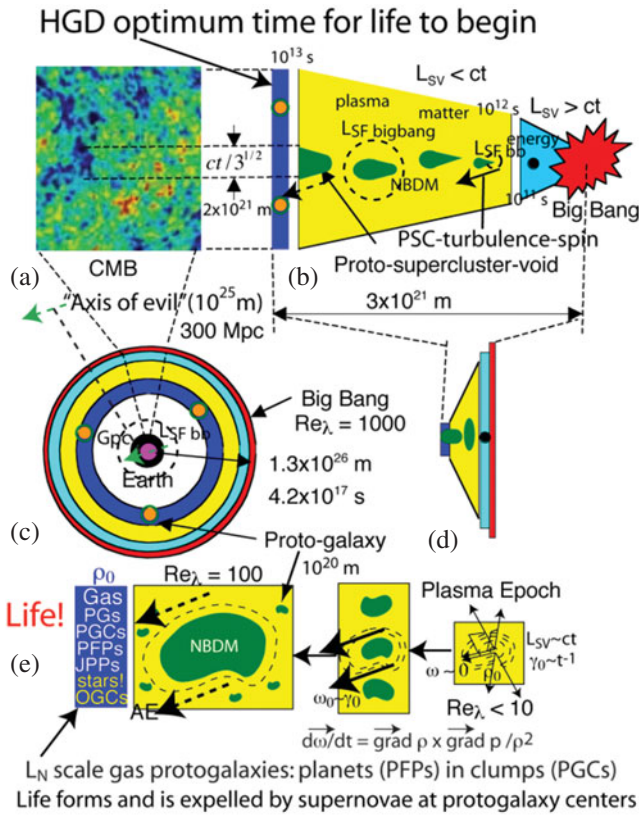


Fig. 4. Early formation of gravitational structures supporting life according to HGD. At plasma-to-gas transition the entire baryonic plasma Universe fragments at the gas Schwarz viscous scale L_{SV} to form planets in clumps within proto-clusters and PSCs of proto-galaxies.

many astronomical sources (Witt & Schild 1988; Furton & Witt 1992; Perrin *et al.* 1995), including the Red Rectangle, is readily explained on the basis of biological pigments as shown by comparing the curves in Fig. 3(b(i) and (ii)). The biological aromatic model for ERE was first proposed by Hoyle & Wickramasinghe (1996) and still remains a valid explanation for this data. The competing models involving inorganically generated PAHs are not as satisfactory, in our view.

Biological aromatic molecules could also be shown to provide an elegant fit to the 2175 Å interstellar extinction feature, both in our galaxy and in external galaxies (Hoyle & Wickramasinghe 2000). Figure 3(b(iii)) shows a comparison between the data for the gravitationally lensed galaxy SBS0909+522 at red shift 0.83 (Motta *et al.* 2002) with the prediction for biological aromatics (Wickramasinghe *et al.* 2009). This latter comparison shows clearly that biological degradation products from disintegrating planets could be detected up to very high redshifts, in this case when the Universe was half its present radius.

In the following we first compare the HGD and Λ CDMHC cosmological models, emphasizing aspects that affect the formation and transmission of life. We then examine the observational evidence, and provide discussion and conclusions.

Hydro-gravitational dynamics versus the standard cosmological model

The standard dark-energy CDM hierarchical-clustering (Λ CDMHC) model of cosmology is modified by modern fluid mechanics to produce the HGD cosmological scenario of Fig. 4.

The key difference between HGD and Λ CDMHC is rejection by HGD of the Jeans 1902 sonic criterion for plasma gravitational structure formation in favour of photon viscosity (Gibson 1996, 2000, 2008). CDM condensations are unnecessary and indeed physically impossible. The Jeans length scale $L_J = V_S t$ is larger than the scale L_H of causal connection ct throughout the plasma epoch, but the Schwarz viscous length scale L_{SV} becomes smaller than ct at a time of only 30 000 years (10^{12} s), which is the time of the first gravitational structure formation by fragmentation to form PSC voids and PSCs.

Vorticity and weak turbulence at the expanding supervoid boundaries determines the morphology of plasma proto-galaxies formed just before the transition to gas (Gibson & Schild 2009). Fragmentation of proto-galaxies occurs along plasma vortex lines at Nomura scales (10^{20} m) and morphology (Nomura & Post 1998) to form chain-galaxy clusters (CGCs) that are clearly visible in the HST ultra-deep field images (Elmegreen *et al.* 2005) and the Tadpole galaxy merger (Gibson & Schild 2002). The NBDM particles (neutrinos) shown in green (Fig. 4e) diffuse to fill the expanding voids and expanding plasma (the neutrino mass is estimated by Nieuwenhuizen (2009)). Fossils of the turbulent big-bang epoch include spin at the strong-force freeze-out scale L_{SF} , stretched from metre scales at the end of inflation to $> ct$ until after the plasma epoch. The plasma density, $\rho_0 = 4 \times 10^{-17} \text{ kg m}^{-3}$, at the time of the first gravitational fragmentation, 10^{12} s, is preserved as the density of globular star clusters (GCs), and the initial fragment mass scale, $\rho_0 (ct)^3$, of a thousand galaxies ($3 \times 10^{45} \text{ kg}$) is preserved as the baryonic mass of galaxy superclusters.

A turbulent big-bang instability occurs at Planck scales, where gravitational, inertial-vortex and centrifugal forces produce the first turbulent combustion by extracting mass energy from the vacuum by stretching turbulent vortex lines until the turbulence power is enhanced exponentially by gluon viscosity and the appearance of the first quarks (Gibson 2004, 2005). Vortex line stretching produces inflation to metre scales at Planck densities with an extraction of big-bang mass energy some 40 orders of magnitude larger than the mass energy observable in our horizon $L_H = ct$, where c is the speed of light and t is the time since the big-bang event. Because temperatures were so high, little entropy was produced except by the turbulence¹. The resulting expansion and

¹ Turbulence (Gibson 1991, 2006) is defined as an eddy-like state of fluid motion where the inertial-vortex forces of the eddies are larger than any other forces that tend to damp the eddies out. Turbulence by this definition always cascades from small scales to large, starting at the viscous inertial-vortex Kolmogorov scale at a universal critical Reynolds number. The mechanism of this ‘inverse’ cascade is the

cooling of the big-bang Universe has a long time constant before the inevitable ‘big crunch’ return of the extracted energy to the vacuum. Fossil turbulence² patterns of the big bang are frozen as the exponentially expanding Universe carries structures to scales separated by distances exceeding L_H , also termed the scale of causal connection, since the maximum speed of gravitational information transport is the speed of light. Because galaxy patterns observed in opposite directions are identical and outside each other’s horizon, this suggests an inflationary expansion period followed the big bang.

Turbulence motions of the big bang have produced unambiguous fossil turbulence fingerprints in the temperature anisotropy patterns observed by cosmic microwave background (CMB) space telescopes (Bershanskii & Sreenivasan 2002, 2003; Bershanskii 2006; Gibson 2010).

The density and rate of strain of the plasma at transition to gas at 300 000 years (10^{13} s) are preserved as fossils of the time of first structure at 30 000 years (10^{12} s), as shown in Fig. 4(e). The plasma turbulence is weak at transition, so the Schwarz viscous scale $L_{SV}=(\gamma\nu/\rho G)^{1/2}$ and Schwarz turbulence scale $L_{ST}=\varepsilon^{1/2}/(\rho G)^{3/4}$ are nearly equal, where γ is the rate of strain, ν is the kinematic viscosity, ε is the viscous dissipation rate and ρ is the density. Because the temperature, density, rate of strain, composition and, thus, kinematic viscosity of the primordial gas are all well known, it is easy to compute the fragmentation masses to be that of proto-galaxies composed almost entirely of 10^{24} – 10^{25} kg planets in million solar-mass 10^{36} kg (PGC) clumps (Gibson 1996). The NBDM (neutrinos) diffuse to diffusive Schwarz scales, $L_{SD}=(D^2/\rho G)^{1/4}$, that are much larger than L_N Nomura scale proto-galaxies, where D is the large NBDM diffusivity with $D\sim\nu$. The rogue-planets prediction of HGD was independently predicted (Schild 1996) by interpretation of a long series of careful quasar microlensing observations that have since been refined and confirmed, and extended, to show the planet mass objects must be in dense clumps.

The optimum time-of-life formation in our favoured HGD cosmology is after the plasma-to-gas transition when the first stars result by binary accretion of primordial planets. Life-forming chemicals occur first near proto-galaxy centres, where strong tidal forces cause turbulence and supernovas of large short-lived stars at turbulent Schwarz scales, $L_{ST}=\varepsilon^{1/2}/(\rho G)^{3/4}$. At this time most of the baryonic matter in

merging of adjacent vortices with the same spin due to induced inertial-vortex forces that force eddy mergers at all scales of the turbulence. Such eddy mergers account for the growth of turbulent boundary layers, jets and wakes. A myth of turbulence theory is that turbulence cascades from large scales to small. It never does, and could not be universally similar if it did. Irrotational flows cannot be turbulent by definition. In self-gravitational fluids, such as stars and planets, turbulence is fossilized in the radial direction by buoyancy forces. Radial transport is dominated by fossil turbulence waves and secondary (zombie) turbulence and zombie turbulence waves in a beamed, radial, hydrodynamic-maser action.

² Fossil turbulence (Gibson 1981, 1986, 1991, 1999) is a perturbation in any hydrophysical field caused by turbulence that persists after the fluid is no longer turbulent at the scale of the perturbation.

the Universe would be in the form of heavy-element enriched primordial planets, with the typical separations between planets $\sim 10^{14}$ m, based on their mass and the gas density.

The onset of prebiotic chemistry and the emergence of life templates as a culmination of such a process must await the condensation of water molecules and organics first into solid grains and thence into planetary cores (Wickramasinghe *et al.* 2010a). Assuming the collapsing proto-planet cloud keeps track with the background radiation temperature, this can be shown to happen between ~ 2 – 30 My after the plasma to neutral transition. With radioactive nuclides ^{26}Al and ^{60}Fe maintaining warm liquid interiors for tens of My, and with frequent exchanges of material taking place between planets, the entire Universe would essentially constitute a connected primordial soup.

Life would have an incomparably better chance to originate in such a cosmological setting than at any later time in the history of the Universe. Once a cosmological origin of life is achieved in the framework of our HGD cosmology, exponential self-replication and propagation continues, seeded by planets and comets expelled to close-by proto-galaxies. Figure 5 contrasts biological processes likely in HGD versus Λ CDMHC cosmologies. The timelines for major events shown in Fig. 5 are very different, so the flood of new information coming from new space and ground-based telescopes is rapidly falsifying the Λ CDMHC. Both cosmologies assume a big-bang initial event. Irrotational, ideal fluid, frictionless flow and adiabatic quantum fluctuations are assumed by the standard model, but HGD requires specific turbulence and fossil turbulence patterns with spin, and is supported by observations (Gibson 2009a, b).

As shown in Fig. 5, HGD conditions for life formation and transmission are optimum immediately after the first stars form and the first stars explode, soon after the plasma-to-gas transition. Because the first stars of Λ CDMHC are superstars that reionize the gas to plasma, and because planets and comets are produced in small numbers only after billions of years, life formation and intergalactic transmission of life templates by panspermia become highly unlikely. Big-bang turbulent friction produces entropy and therefore a big crunch, rather than the open Universe expected if one assumes cosmological constant dark energy (Λ), with big-bang-turbulence and gluon-viscous dark energies (Λ_{HGD} as the necessary anti-gravity forces of the big bang.

Unequivocal proof that planets in clumps are the source of all stars and the dark matter of galaxies is difficult to obtain. The nearest primordial planet to a star is about 5×10^{15} m, the distance to the Oort ‘cloud’ of comets, representing the inner surface of the Oort cavity within a PGC clump produced when merging planets form a central star. Since the primordial planets are the mass of the Earth with the average density of frozen hydrogen, the angular size of the planet from Earth is only $\sim 2 \times 10^{-10}$ radians.

Unfortunately, this is $\sim 0.1\%$ the resolution of the HST. When objects, such as dying stars, begin to spin up and radiate, the dark matter planets come out of the dark because radiation can produce large gaseous atmospheres.

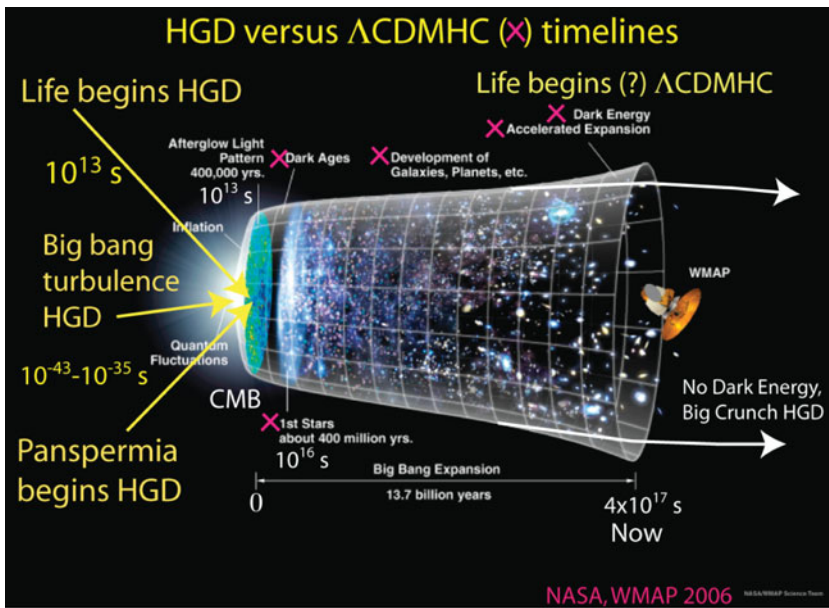


Fig. 5. Contrast between HGD and Λ CDMHC timelines for gravitational structures, and for life formation and panspermia. If abiogenesis can work in a time period of a few million years, then all the necessary chemicals, comfortable environments and means of dispersal of the resulting life templates are provided by HGD soon after the plasma-to-gas transition at 10^{13} seconds. Harsh early conditions of the standard model and its lack of primordial planets make life formation rare and more difficult to disperse.

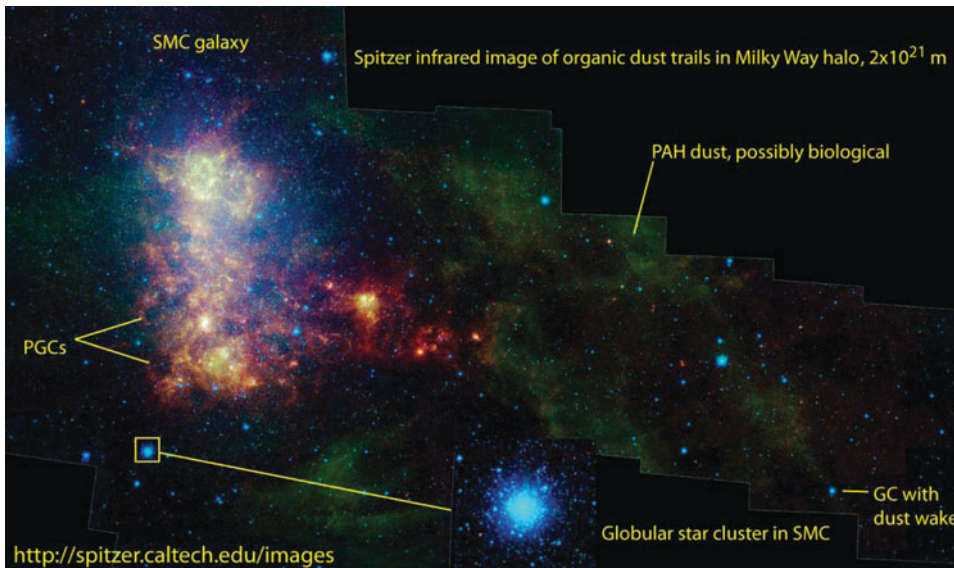


Fig. 6. Spitzer infrared telescope image of the SMC galaxy at a distance of 70 kpc ($\sim 2 \times 10^{21}$ m). Dark-matter PGCs with fragmentation scale $(M/\rho_0)^{1/3} \sim 4 \times 10^{17}$ m show PAH dust-wake evidence of life occurs only occasionally at PGC scales, and sometimes not at all, as seen for the SMC GC (bottom insert).

The nearest planetary nebula to the Earth is the Helix (Figs 1–3), where thousands of planetary objects have been observed by optical and infrared telescopes because their atmospheres have expanded to sizes up to $\sim 10^{13}$ m. Radiation is caused by planet accretion and the rapid spinning of the white dwarf, pumping a powerful plasma jet that partially evaporates frozen gas planets at the inner boundary of the Oort cavity (Gibson 2009b, p. 114, Fig. 11).

Because dark matter planets are much colder than stars, they are easier to see in the infrared frequency band

than in the optical. Only ~ 5000 planets can be seen in Helix (Figs 1–3) at optical frequencies by the HST, but $\sim 40\,000$ were detected in the infrared by the Spitzer telescope (Fig. 1).

Figure 6 is an infrared Spitzer image of the Small Magellanic Cloud (SMC). Possibly biological PAH dust wakes (green) appear behind some of the numerous globular star clusters (GCs), but not all. Dark PGCs with PAH dust appear (on the left-hand side) in the SMC from optical backlighting with their primordial fragmentation scale

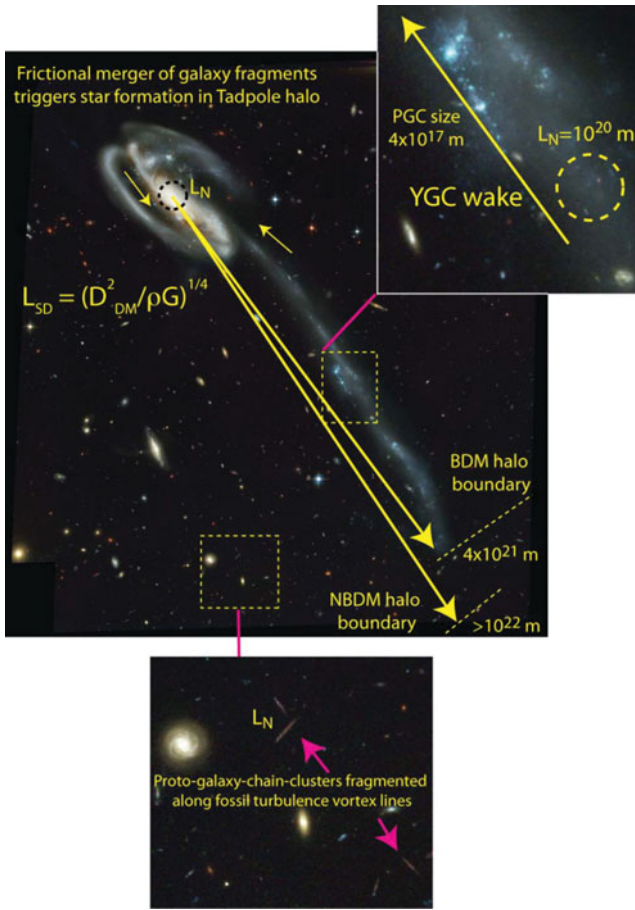


Fig. 7. Tadpole galaxy merger brings the BDM halo out of the dark. Nomura-scale galaxy fragments trigger star formation (right insert) in young GCs (YGCs). Tran *et al.* (2003) identify 42 YGCs, precisely aligned along the star wake path towards frictional mergers of the fragments (Gibson 2008). Schwarz diffusive scales, L_{SD} , are shown for the baryonic and NBDM diffused from the L_N -scale proto-galaxy to form BDM and NBDM halos. Background CGCs are fragmented at L_N scales along fossil-turbulence vortex lines of the plasma epoch.

4×10^{17} m, matching the GC size (centre insert). The SMC clump of PGCs is well within the 10^{22} m diameter PGC dark matter halo of the Milky Way expected from HGD (and as observed, see Fig. 7).

Theory and observations

Important concepts missing in discussions leading to the standard cosmological model (Peacock 2000) are the absolute instabilities of turbulence, gravity and living processes. Starting from an initial condition at rest with small density fluctuations, structures will form in a gravitational free fall time $\tau_g = (\rho G)^{-1/2}$, where G is Newton’s gravitational constant. Within a horizon length ct , mass will immediately start to move away from density minima and towards density maxima with exponentially increasing acceleration and viscous dissipation as the time approaches τ_g . In an expanding

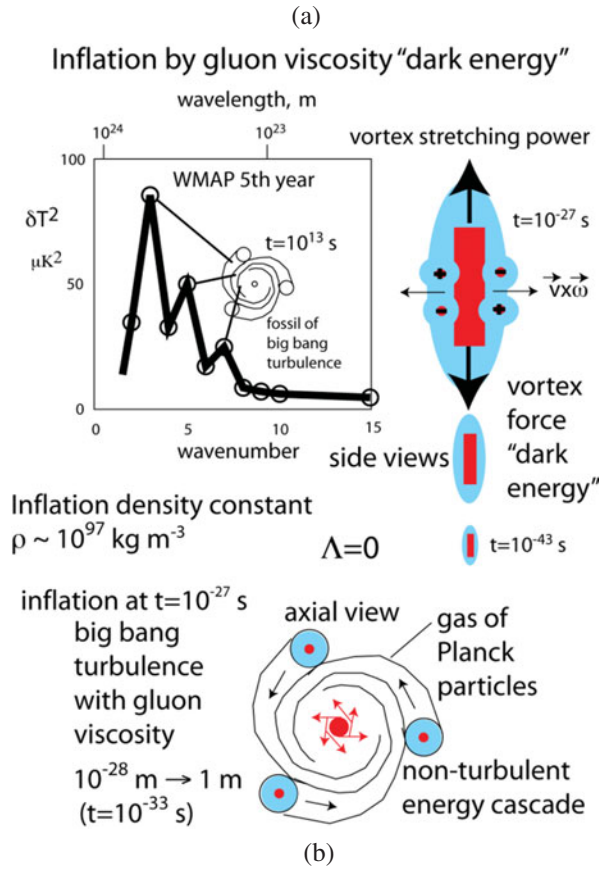


Fig. 8. Evidence for big-bang turbulence-driven inflation appears at the smallest wavenumber (largest scale) temperature anisotropies observed by the WMAP fifth microwave background telescope team (a), interpreted here as a fossil of a non-turbulent kinetic energy cascade induced by big-bang turbulent vortices (b).

universe the formation of voids is favoured, as shown in Fig. 4(b), (d) and (e).

The baryonic plasma density falls to near zero within a PSC void within 10^{12} s and the void expands driven by gravity as a rarefaction wave limited by the sound speed, $V_s = c/3^{1/2}$, in the plasma until the plasma-to-gas phase change at 10^{13} s. This is the HGD interpretation of the primary sonic peak with angular size of about one degree observed by Wilkinson microwave anisotropy probe (WMAP) and other microwave background telescopes. The 0.4° and 0.2° sonic peaks are interpreted as wrapping, by fossil big-bang turbulence spin, of secondary turbulence vortex lines, around the boundaries of the expanding PSC voids (Gibson 2010).

A preferred spin direction has been identified on the sky, towards which x-ray galaxy clusters are moving and towards which point the spin axes of the Milky Way and our local galaxies. It is also the direction of all low wavenumber spherical harmonic wave vectors of the CMB (Schild & Gibson 2008). It explains large extragalactic magnetic fields detected at supercluster-void scales (10^{25} m, 300 Mpc) by the Fermi γ -ray space telescope (Novronov & Vovk 2010) as TeV γ -ray interactions with B-fields in large rotating voids expected from HGD but not Λ CDMHC.

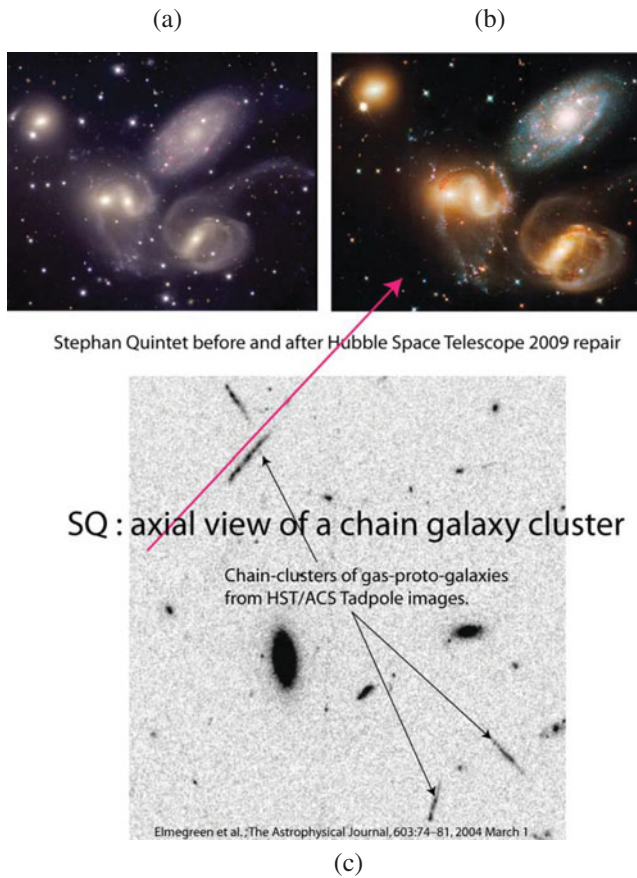


Fig. 9. Evidence that galaxies form as CGCs along plasma-epoch turbulent vortex lines is provided by Stephan’s Quintet. The repaired HST ACS3 and spectrometer (a) make the blue shift of the nearest galaxy obvious, as well as the interpretation (Gibson 2009a, b) that Stephan’s Quintet (SQ) is a CGC axial view. Four CGC side views (b) appear in the HST image of the Tadpole galaxy merger.

To describe big-bang turbulent combustion and inflation requires the discussion of some basic properties of turbulence and fossil turbulence at the beginning of time (Gibson 2004, 2005). Newtonian gravitation is modified by relativistic effects where pressures are of order ρc^2 and may be enormously negative from the effects of the induced non-turbulent energy cascade of Planck gas and radial viscous and anti-gravity turbulent inertial-vortex forces, as shown in Fig. 8, particularly at the strong force freeze-out phase change, where the Planck fireball cools from the Planck temperature of 10^{32} K to 10^{28} K so that quarks and gluons (which transmit strong forces) become possible.

The big-bang turbulent combustion instability is extremely efficient and breaks symmetry for the universe created with the first prograde accretion of a Planck anti-particle and a spinning Planck particle-antiparticle pair. From the Kerr metric, 42% of the rest mass energy of each prograde accretion is converted from gravitational potential energy to the production of more Planck particles (Peacock 2000, p. 61, eq. 2.106), always retaining a slight statistical bias toward the production of matter rather than antimatter in the big-bang remnants.

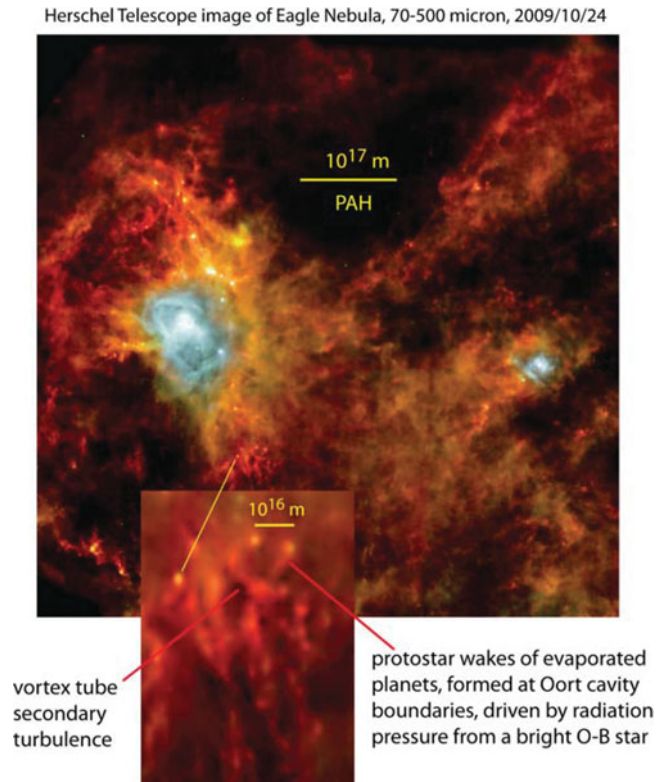


Fig. 10. Herschel space telescope image from the Eagle star-forming region (box in Fig. 11). Bright infrared objects in the bottom insert are interpreted as large planets and brown dwarf protostars with warm Earth-mass planet wakes evaporated at smaller Oort cavity boundaries than those shown in Fig. 1(a) and (b). The dark PAH-obscured region at the top is interpreted as a PGC clump of strongly life-infected planets, reduced in size and distorted by the strong turbulence of this star-forming region.

During inflation, the expansion of space does work by stretching Planck–Kerr vortex lines and (Fig. 8(a)) opposing gluon-viscous stresses, exponentially creating yet more space–time and mass energy. Secondary turbulent vortices wrap around the central vortex tube with alternating spin directions, creating powerful anti-gravity inertial-vortex-force and gluon-viscosity ‘dark energy’. Gluons are the fundamental particles (bosons) that transmit the strong force that binds quark particles together in an atomic nucleus. Larger-scale momentum transport from free gluons within the quark gluon plasma vastly increases the viscosity of the big-bang fireball, converts total pressure from positive to negative and powers exponential inflation of space and mass energy (Fig. 8(b)). The exponentially increasing negative power is balanced by exponentially increasing mass energy during inflation, keeping constant mass-energy density near its Planck value of 10^{97} kg m⁻³. Turbulent dissipation rates are high, but little entropy is produced at Planck temperatures 10^{32} K decreasing to 10^{28} K at strong-force freeze out. Thus, the turbulent big-bang powered inflationary expansion of space is nearly adiabatic (flat) and will remain so for some time before its inevitable collapse.

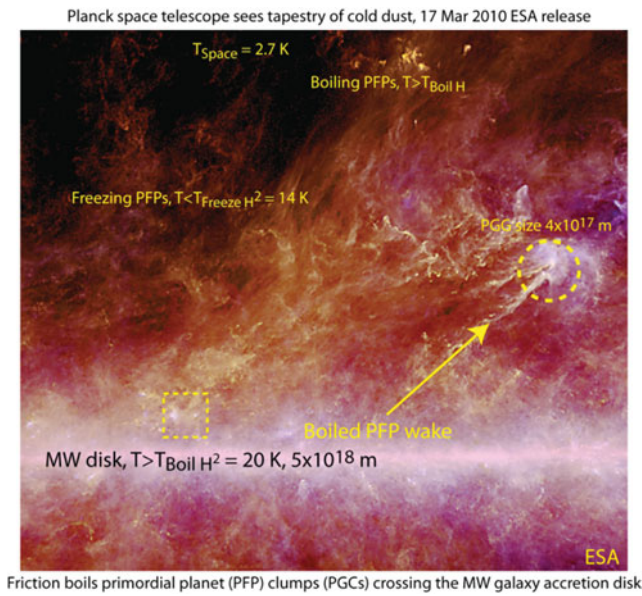


Fig. 11. Planck telescope European Space Agency release image from 17 March 2010. Measured temperatures reveal PGC wakes of merged planets triggered into formation by the PGC centre of gravity as it moves through the Milky Way disk, as shown by the arrow. Figure 6 from the dashed box star-forming region shows evidence from PAH dust of turbulent mixing, resulting in the smaller size of the PGCs.

For the combustible fluid of turbulent Planck particles and quark-gluon plasma of Fig. 8, the energy momentum tensor of Einstein’s field equations is proportional to a frictional lost-work term (anti-gravity turbulent and gluon-viscosity ‘dark energies’) rather than the inviscid, adiabatic term Λ , the Einstein cosmological constant. The source of anti-gravity is the turbulent inertial-vortex forces of adjacent vortex lines of opposite spin in the Planck gas surrounding the central vortex, stretched out in pairs with opposite spin, like the streamwise vortices of Langmuir cells in a wind-driven boundary layer or the wingtip vortices of an airplane. Such forces cause smoke rings and wingtip vortices to translate and expand, and cause adjacent vortices with the same spin to merge. Stretching vortex lines in tornadoes and hurricanes accounts for the cascade of turbulent kinetic energy from small scales to large in these vortex structures, feeding on the induced non-turbulent kinetic energy cascade from large scales to small.

Figure 9 shows recent infrared HST evidence (Fig. 9(b)) of vortex-line chain clusters seen axially in Stephan’s Quintet and in side view (Fig. 9(c)). See Fig. 7 for the Tadpole image.

The Herschel space telescope and the Planck space observatory were launched on 14 May 2009, and are now providing high-resolution infrared images from orbits at the second Lagrange point $1.5 \times 10^{12} \text{ m}$ from Earth. Figure 10 shows one of the first Herschel images, from the Eagle star-forming region of the Milky Way PGC accretion disk.

The Eagle star-forming region is in the partially turbulent, stably stratified Milky Way accretion disk formed as frozen PGCs evaporated from the 10^{20} m Nomura-scale

proto-galaxy core into the 10^{22} m diameter dark-matter halo accrete on the disk plane. Figure 11 is a recent Planck space observatory image of what is described as a ‘tapestry of cold dust’. The Herschel image of Fig. 10 is from the region shown by the dashed yellow box at lower left of Fig. 11, just above the disk.

Remarkably, the dust temperatures of Fig. 11 are close to the 14–20 K freezing–boiling points of hydrogen, suggesting frictional forces of the accretion disk are responsible for evaporating the frozen planets of the PGC traversing the disk. Figure 12 shows an infrared Herschel image of the optically dark ‘coalsack’ dark cloud in the Crux southern hemisphere constellation (bottom insert).

We consider these few infrared space telescope images to be only the first trickle in a future flood of information relevant to HGD predictions about the origin of life from primordial planets.

Discussion

An accumulation of evidence in a variety of frequency bands from a variety of very high resolution and highly sensitive modern telescopes supports the hypothesis that the dark matter of galaxies is primordial planets in PGC clumps, as predicted from HGD (Gibson 1996) and inferred from quasar microlensing (Schild 1996). All stars form from these planets so all star models and planetary nebulae models must be revised to take the effects of planets and their brightness and dimness into account. Figure 13 (Gibson 2010, Fig. 1) shows evidence of PGCs as the dark matter of the Milky Way Galaxy in a variety of frequency bands, from microwave to infrared (Veneziana *et al.* 2010). The diffuse infrared background explorer (DIRBE) image permits a planet-mass estimate exceeding that of stars.

Figure 13 leaves little room for doubt that the dark matter of the Milky Way Galaxy is made up of PGC clumps of frozen hydrogen planets. The ‘cirrus clouds of dust’ (Veneziana *et al.* 2010 and other authors) are suspiciously warm in the range of triple-point temperatures of frozen and boiling hydrogen expected if the ‘dust’ of the cirrus clouds is planets in the Earth to Jupiter mass range, caused to change phase by their close proximity in planetary nebulae to stars formed by the planets within the planet clumps, and fed to dangerously large masses by a constant diet of comets now made visible by the new infrared space telescopes in Figs 1–3. A surprising discovery of a significant excess millimetre to submillimetre spectral emission of unknown nature from the large and SMCs (Israel *et al.* 2010) implies massive (PGC) clumps of cold ‘dust’ (primordial planets).

Figure 7 is the Tadpole galaxy merger (UGC 10214, VV29) HST archive high-resolution image, clearly showing merging galaxy fragments on a frictional track through the baryonic dark matter (BDM) halo. Galaxy VV29a, in the head of the Tadpole, has the usual Nomura-scale L_N of OGCs reflecting the size of its proto-galaxy. As the PGC clumps of planets freeze the planets and clumps become increasingly collisionless and diffusive, forming the L_{SD} -scale BDM halo expanded

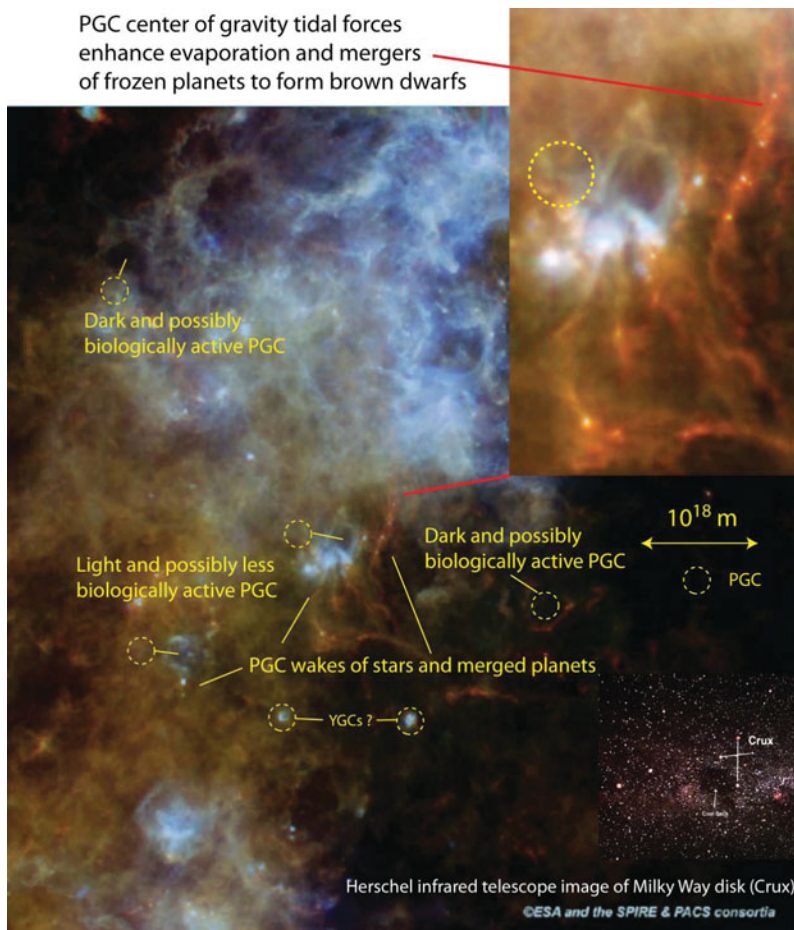


Fig. 12. Herschel space observatory infrared image of the optically dark ‘coalsack’ in the Crux region of the Milky Way disk. PGC scales are shown by dashed circles. Some are dark and some are light. Many are fringed by brightness and show wakes of bright clumps suggesting enhanced PFP planet mergers to form larger planets and gravitationally heated mini-brown-dwarf stars. Darkness and brightness of the PGC clumps is interpreted as PAH evidence of biological activity.

by a factor of 80 in its radius. The NBDM halo (neutrinos) diffuses to a much larger radius. Even though the NBDM has ~ 30 times more mass than the BDM, its contribution to the central galaxy density is small.

Turbulence produces post-turbulence remnants (fossil turbulence) with structure in patterns that preserve evidence of previous events, such as big-bang turbulence and plasma-epoch turbulence. Fossil-turbulence perturbations (Gibson 1981) guide the evolution of all subsequent gravitational structures. Numerous fatal flaws in the standard Λ CDMHC cosmology have appeared that can be traced to inappropriate and outdated fluid mechanical assumptions (Jeans 1902) that can be corrected by HGD (Gibson 1996; Schild 1996; Gibson & Schild 1999a, b, 2002, 2007a, b; Schild & Gibson 2008). Critically important advances in the understanding of fluid mechanics are the correct definitions of turbulence and fossil turbulence and the realization that all turbulence cascades from small scales to large (Gibson 1986, 1991, 2006).

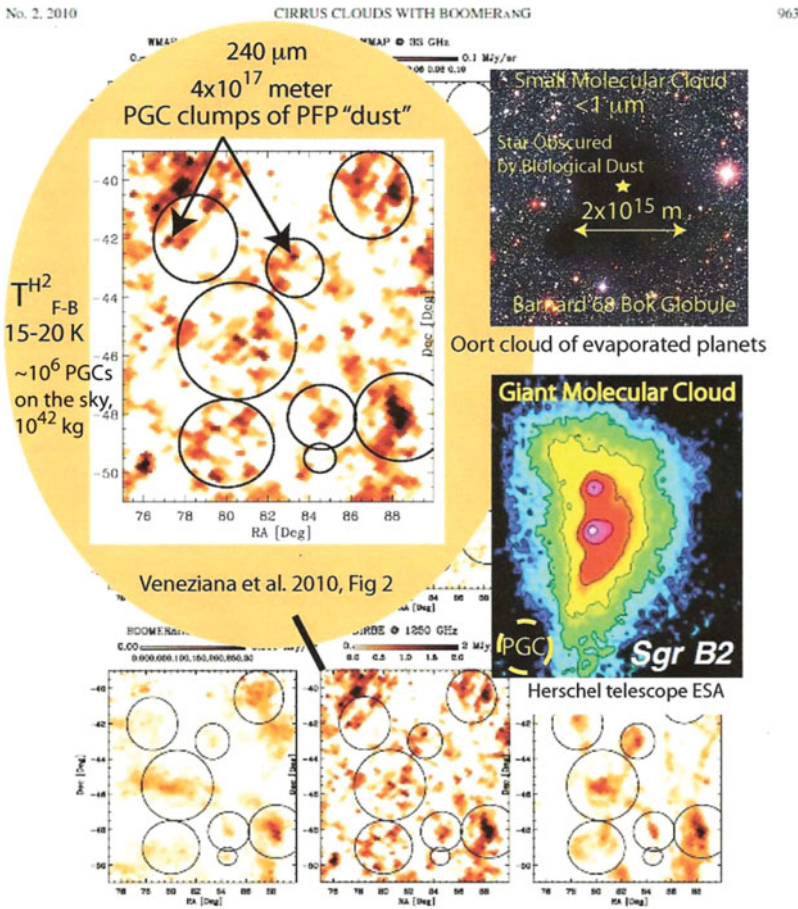
Failure to understand these advances has also hampered fields of oceanography and atmospheric science, which have not yet recognized the importance of fossil turbulence, fossil turbulence waves, zombie turbulence and zombie turbulence

waves as dominant physical mechanisms of terrestrial radial transports of hydrophysical fields, and for the preservation of information about previous turbulence (Keeler *et al.* 2005; Gibson *et al.* 2006, 2008). Enormous undersampling errors are characteristic of equatorial turbulence estimates in both the ocean and atmosphere from the same extreme lognormal intermittency factors that have prevented the massive compact halo object (MACHO), Earth resources observation system (EROS) and optical gravitational lensing experiment (OGLE) microlensing consortia from detecting primordial planets as the BDM of galaxies (Gibson & Schild 1999a, b). Figure 14 shows the effect of such undersampling errors on the EROS (Renault *et al.* 1997) MACHO exclusion diagram.

As shown in Fig. 14, the EROS-1 collaboration expected 20–50 microlensing events from Large Magellanic Cloud (LMC) and SMC star sources and saw none. However, all the Galaxy models of all the collaborations neglect the statistical effects of intermittent lognormal probability distributions (Gibson & Schild 1999b).

We have seen that the enormous numbers of planets required by hydro-gravitational dynamics have major biological consequences. Because planets in clumps are

“Dust” temperatures match hydrogen-planet Freezing-Boiling points



Gibson 2010 Fig. 1, arXiv:1005.2772

Fig. 13. Microwave background images (Veneziana *et al.* 2010, Figs 1 and 2) from many platforms show redundant images of ‘cirrus dust clouds’ with ‘dust’ temperatures matching frozen hydrogen planet freezing–boiling temperatures $T_{FB} = 15\text{--}20\text{ K}$. The DIRBE $240\ \mu\text{m}$ image (orange oval) indicates $\sim 10^6$ PGC ‘dust’ clumps similar to the Sgr B2 gmC (right centre). A small molecular cloud in the visible suggests biological dust ejected from evaporated hydrogen planets surrounding an Oort cavity (right top).

primordial components of dense and warm proto-galaxies in proto-galaxy clusters, it seems likely that the first life forms were also primordial. Because the efficiency of producing life from seeds is so much greater than producing life from inorganic chemical soups, it seems clear that the carbon-based life forms observed on Earth reflect a cosmic ecosystem beginning soon after the plasma-to-gas transition, following the formation and death of the first stars. OGCs show that the first stars were likely formed in a very gentle Universe of warm gassy planets. The stars died when their overfed carbon cores exploded as SNe Ia events, giving the carbon, oxygen, calcium, nitrogen and other basic chemicals of life as we know it. Signatures of life on other planets are rapidly becoming abundant in the new infrared and radio telescope images. The amazing diversity and complexity of organic molecules found in the older-than-Earth Murchison meteorite (Schmitt-Kopplan *et al.* 2010) and in the interstellar medium could, in our model, represent the disruption of biology and its waste products and nutrients from disintegrating frozen planets and comets.

In view of the grotesquely small improbability of the origin of the first template for life (Hoyle & Wickramasinghe 1982) it is obvious that it would pay handsomely for abiogenesis to embrace the largest available cosmic setting. The requirement is for a connected set of cosmic domains where prebiology and steps towards a viable set of life templates could take place and evolve. In the present HGD model of cosmology the optimal setting for this is in events that follow the plasma-to-gas transition 300 000 years after the big bang. A substantial fraction of the mass of the entire Universe at this stage will be in the form of frozen planets, enriched in heavy elements, and with radioactive heat sources maintaining much of their interior as liquid for some million years. The close proximity between such objects (mean separations typically 10–30 AU) will permit exchanges of intermediate templates and co-evolution that ultimately leads to the emergence of a fully fledged living system. No later stage in the evolution of the Universe would provide so ideal a setting for the *de novo* origination of life. When re-frozen primordial planets are disrupted in the

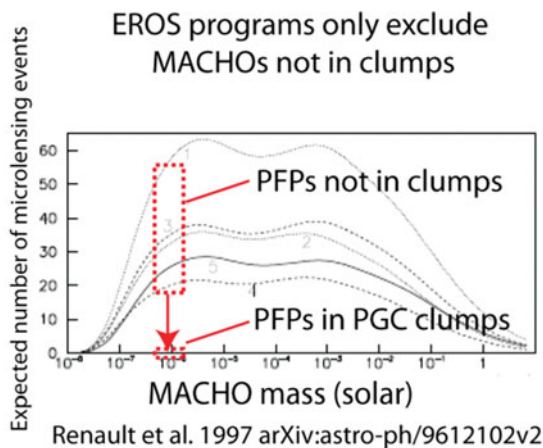


Fig. 1. Expected number of microlensing events in the EROS programs (CCD-LMC and SMC sources- and Schmidt plates) assuming that all Galactic dark matter is in the form of machos of the same mass. The five curves refer to the Galaxy models of table 1. The full curve corresponds to the reference model, dashed curves to flattened models and dotted curves to the spherical models.

The expected number of events is reduced by extreme intermittency factors that arise in the nonlinear accretional cascade of PFP planets to form stars within PGC clumps (Gibson & Schild 1999b)

Fig. 14. Exclusion diagrams of the MACHO, EROS, and OGLE microlensing collaborations overestimate the number of events to be expected by assuming the MACHO objects (e.g. PFP planets) are not clumped.

vicinity of stars within galaxies, panspermic dispersal of life occurs.

Figure 15 is a collection of microscopic images of materials from comets and their fragments in the form of meteors and meteor dust (Wickramasinghe *et al.* 2010). It seems obvious from their morphology that these are fossil remains of life. The Murchison meteorite is claimed to be older than the Earth, so the fossilized life is apparently extraterrestrial.

Conclusions

We conclude that standard models for the evolution of structure in the Universe and standard models for the formation of life on Earth cannot be reconciled with the flood of new evidence from modern telescopes. The standard dark-energy-CDM (Λ CDMHC) model is fatally flawed, doomed to failure by incorrect assumptions of collisionless, ideal, frictionless fluids and non-turbulent fluid motions. Modern concepts of turbulence, fossil turbulence, fossil turbulence waves and stratified turbulent transport result in vast differences between predictions for the formation of the Universe, and the formation, evolution and morphology of gravitational structures with time. HGD and Λ CDMHC cosmologies are contrasted in Fig. 4. HGD lead immediately to conditions most favourable to the origin of life and its cosmic transport.

Primordial planet formation in clumps at the plasma-gas transition is the most important result of HGD

cosmology with respect to the emergence of life on Earth. The planets merge to form stars, and pieces of planets form moons and comets as venues and vectors for life. Mergers of nearby primordial planets and their fragments are manifested by long-duration radio transients, lacking optical counterparts, occurring with energies exceeding a Jansky 10^5 times a year (Ofek *et al.* 2010) at distances from 10^{18} to 10^{20} m, more than that needed for simple binary mergers of planets to form Milky Way disk stars. Infrared and other telescopes (Spitzer, Planck, Herschel, HST) should be coordinated in future tests to within the half-hour to several-day duration periods of such events to exploit this potential gold mine of information about the origin of stars and of life.

The abundance and degree of complexity of biologically relevant molecules in dense interstellar clouds are consistent with the degradation of an all-pervasive cosmic biology that originated 300 000 yr after the big bang. Spitzer, Hubble and Subaru space telescope pictures of evaporating planets in Helix PNe in Figs 1–3 show the possible effects of biological waste on planet and comet heat and mass transport processes near a dying star. Dusty (biologically infected) planets grow large atmospheres and are radially ejected by central white dwarf radiation pressure, while less dusty (less biologically infested) planets grow smaller atmospheres from reduced heating and fall into the star as proto-comets, proto-asteroids and evaporated gas formed by friction, tidal interactions and radiation.

PGC clumps of planets with markedly different dust contents can be inferred from Milky Way disk images of infrared telescopes Spitzer and Herschel. We hypothesize that the dust is biological in origin, and that PGC clumps without PCH (oil-like) dust to make them optically opaque are significantly less infected by carbon-based organisms, which rely on such carbohydrates for and polyaromatic hydrocarbons energy. Because frictional agitation of PGCs crossing and entrained by the Galaxy accretion disk is uniform, adequate chemical fertilizer and cosmic seeding to produce life in PGC planets in the disc of the Galaxy should be available. The Planck space telescope more precisely confirms the boiling and freezing point temperatures of dark-matter planets in dense clumps, with and without biological signatures, as the Galaxy dark matter. Summary plots in Figs 7, 13 and 14 overwhelmingly support the HGD claim that the dark-matter missing mass of galaxies is primordial planets in primordial clumps.

It appears that hundreds of millions of years for a planet (such as Earth) in galaxy-disk conditions provides no guarantee that life will occur from abiogenesis. If cosmologically generated primordial life is all-pervasive as we have argued, seeding would be a guaranteed route to life on every habitable planet in the Universe. It would therefore be expected that such life would be present in great profusion in the comets of our own Solar System, and evidence for this may be found in comet dust and in carbonaceous meteorites, which are derived from comets. The montage of images in Fig. 15 shows a sample of microbial fossils in meteorites and comet dust. Biochemical markers corroborate the putative biological identification of these structures (Wickramasinghe

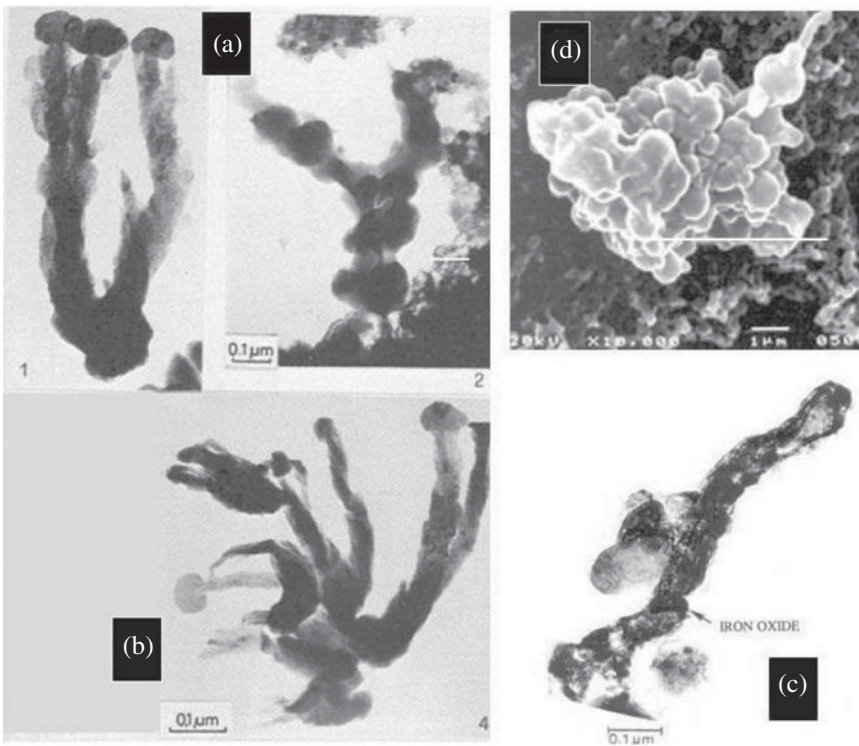


Fig. 15. Microbial fossils in comets. (a), (b) Bacterial microfossils in the Murchison meteorite (courtesy of Hans Pflug). (c) A bacterial fossil within a Brownlee particle. (d) a clump of cocci and a bacillus from dust collected using a cryoprobe from 41 km in the atmosphere. References and credits are given in Wickramasinghe *et al.* (2010).

et al. 2010a, b). Moreover, recent studies indicate that life forms on Earth have made only a modest progress towards achieving the biochemical diversity displayed within the Murchison meteorite, even with the continuing injection of cometary organics and presumably cometary life (Schmitt-Kopplan *et al.* 2010). Life on Earth evidently represents a small subset of the total range of possibilities available in the entire cosmos. A wealth of observational and experimental data now point to the conclusion that life on Earth is derived from the vast cosmos as was proposed decades ago by Fred Hoyle and one of the present authors (NCW) (Hoyle & Wickramasinghe 1982, 2000). In conclusion we note that without comets seeding the Earth with cosmologically derived microorganisms our planet would have remained lifeless and barren to the present day.

References

- Bershanskii, A. (2006). *Phys. Lett. A* **360**, 210–216.
- Bershanskii, A. & Sreenivasan, K.R. (2002). *Phys. Lett. A* **299**, 149–152.
- Bershanskii, A. & Sreenivasan, K.R. (2003). *Phys. Lett. A* **319**, 21–23.
- Bouwens, R.J., Illingworth, G.D., Oesch, P.A., Stiavelli, M., van Dokkum, P., Trenti, M., Magee, D., Labbé, I., Franx, M., Carollo, C.M. & Gonzalez, V. (2010). *Astrophys. J. Lett.* **709**, L133–L137, arXiv:0909.1803v3.
- Elmegreen, D.M. *et al.* (2005). *Astrophys. J.* **631**, 85–100.
- Furton, D.G. & Witt, A.N. (1992). *Astrophys. J.* **386**, 587.
- Gahm, G. *et al.* (2007). *Astrophys. J.* **133**, 1795–1809.
- Gibson, C.H. (1981). *Am. Inst. Aeronaut. Astronaut.* **19**, 1394.
- Gibson, C.H. (1986). *J. Fluid Mech.* **168**, 89–117.
- Gibson, C.H. (1991). *Proc. Roy. Soc. Lond. A* **434**, 149–164.
- Gibson, C.H. (1996). *Appl. Mech. Rev.* **49**(5), 299–315.
- Gibson, C.H. (1999). *J. Mar. Syst.* **21**(1–4), 147–167, astro-ph/9904237.
- Gibson, C.H. (2000). *J. Fluids Eng.* **122**, 830–835.
- Gibson, C.H. (2004). *Flow Turbul. Combust.* **72**, 161–179.
- Gibson, C.H. (2006). *Turbulence, Encyclopedia of Physics*, ed. Lerner, R.G. & Trigg, G.L., pp. 1310–1314. Addison-Wesley Publishing Co., Inc., London, UK.
- Gibson, C.H. (2008). *J. Appl. Fluid Mech.* **1**(2), 1–8, arXiv:astro-ph/0606073.
- Gibson, C.H. (2009a). *New Cosmology: Cosmology Modified by Modern Fluid Mechanics*. Amazon.com, Inc., Seattle, Washington, USA. ISBN 978-1449507657.
- Gibson, C.H. (2009b). *New Cosmology II: Cosmology Modified by Modern Fluid Mechanics*. Amazon.com, Inc., Seattle, Washington, USA. ISBN 978-1449523305.
- Gibson, C.H. (2010). Turbulence and turbulent mixing in natural fluids, *Physica Scripta* Topical Issue, Turbulent Mixing and Beyond (TMBW '09), (in press), arXiv:1005.2772v4.
- Gibson, C.H., Bondur, V.G., Keeler, R.N. & Leung, P.T. (2006). *Int. J. Dyn. Fluids* **2**(2), 171–212.
- Gibson, C.H., Bondur, V.G., Keeler, R.N. & Leung, P.T. (2008). *J. Appl. Fluid Mech.* **1**(1), 11–42.
- Gibson, C.H. & Schild, R.E. (1999a). Quasar-microlensing versus star-microlensing evidence of small-planetary-mass objects as the dominant inner-halo galactic dark matter, arXiv:astro-ph/9904362.
- Gibson, C.H. & Schild, R.E. (1999b). Theory and observations of galactic dark matter, arXiv:astro-ph/9904366.
- Gibson, C.H. & Schild, R.E. (2010). Interpretation of the Tadpole VV29 Merging Galaxy System using Hydro-Gravitational Theory, *Physica Scripta* Topical Issue, Turbulent Mixing and Beyond (TMBW '09), (in press), arXiv:astro-ph/0210583.
- Gibson, C.H. (2005). The first turbulent combustion, *Combust. Sci. and Tech.*, **177**, 1049–1071, arXiv:astro-ph/0501416

- Gibson, C.H. & Schild, R.E. (2007a). Interpretation of the Helix Planetary Nebula using Hydro-Gravitational-Dynamics: Planets and Dark Energy, arXiv:astro-ph/0701474.
- Gibson, C.H. & Schild, R.E. (2007b). Interpretation of the Stephan Quintet Galaxy Cluster using Hydro-Gravitational-Dynamics: Viscosity and Fragmentation, arXiv[astro-ph]:0710.5449.
- Gibson, C.H. & Schild, R.E. (2009). *J. Appl. Fluid Mech.* **2**(2), 35–41, arXiv:0808.3228.
- Gibson, C.H. & Wickramasinghe, N.C. (2010). The imperatives of Cosmic Biology. *J. Cosmol.* (in press), arXiv:1003.0091.
- Hoyle, F. & Wickramasinghe, N.C. (1977). *Nature* **270**, 323.
- Hoyle, F. & Wickramasinghe, N.C. (1982). *Proofs that Life is Cosmic*, Mem. Inst. Fund. Studies Sri Lanka, No. 1 (<http://www.panspermia.org/proofslifeiscosmic.pdf>).
- Hoyle, F. & Wickramasinghe, N.C. (1996). *Astrophys. Space Sci.* **235**, 343.
- Hoyle, F. & Wickramasinghe, N.C. (2000). *Astronomical Origins of Life: Steps towards Panspermia*. Kluwer Academic Press, Frankfurt.
- Israel, F.P. *et al.* (2010). Sub-millimeter to centimeter excess emission from the Magellanic Clouds. 1. Global spectral energy distribution, to be published in *Astronom. Astrophys.* 4 June, arXiv:1006.2232v1.
- Jeans, J.H. (1902). *Phil. Trans.* **199A**, 0–49.
- Keeler, R.N., Bondur, V.G. & Gibson, C.H. (2005). *Geophys. Res. Lett.* **32**, L12610.
- Matsuura M., Speck, A.K., McHunu, B.M., Tanaka, I., Wright, N.J., Smith, M.D., Zijlstra, A.A., Viti, S. & Wesson, R. (2009). *Astrophys. J.* **700**, 1067–1077.
- Meaburn, J. & Boumis, P. (2010). *Mon. Not. R. Astron. Soc.* **402**, 381–385, doi:10.1111/j.1365-2966.2009.15883.x
- Motta, V., Mediavilla, E. & Munoz, J.A. (2002). *Astrophys. J.* **574**, 719.
- Nieuwenhuizen, T.M. (2009). *Europhys. Lett.* **86**, 59001, arXiv:0812.4552.
- Nieuwenhuizen, T.M., Gibson, C.H. & Schild, R.E. (2009). *Europhys. Lett.* **88**, 49001.
- Nomura, K.K. & Post, G.K. (1998). *J. Fluid Mech.* **377**, 65–97.
- Novronov, A. & Vovk, I. (2010). *Science* **328**, 73–75.
- Ofek, E.O. *et al.* (2010). *Astrophys. J.* **711**, 517–531.
- Peacock, J.A. (2000). *Cosmological Physics*. Cambridge University Press, Cambridge.
- Peebles, P., James, E., Lyman, A., Page, R. Jr. & Partridge, B. (2009). *Finding the Big Bang*. Cambridge University Press, Cambridge.
- Perrin, J.M., Darbon, S. & Sivan, J.P. (1995). *Astronom. Astrophys.* **304**, L21–25, arXiv:astro-ph/9512046v1.
- Renault, C. *et al.* (EROS-1 coll.) (1997). *Astronom. Astrophys.* **324**, L69, astro-ph/9612102v2.
- Schild, R. (1996). *Astrophys. J.* **464**, 125.
- Schild, R.E. & Gibson, C.H. (2008). Lessons from the Axis of Evil, arXiv[astro-ph]:0802.3229v2.
- Schmitt-Kopplan, P. *et al.* (2010). *Proc. Nat. Acad. Sci.* **107**(7), 2763–2668.
- Tran, H.D. *et al.* (2003). *Astrophys. J.* **585**, 750.
- Veilleux, S. *et al.* (2009). *Astrophys. J. Suppl.* **182**, 628–666, doi:10.1088/0067-0049/182/2/628.
- Veneziana, M. *et al.* (2010). Properties of Galactic Cirrus Clouds observed by Boomerang, arXiv:0907.5012v2.
- Weinberg, S. (2008). *Cosmology*. Oxford University Press, Oxford.
- Wickramasinghe, C. (2005). *A Journey with Fred Hoyle, The Search for Cosmic Life*. World Scientific Publ., Singapore.
- Wickramasinghe, C. (2010). *Int. J. Astrobiol.* **9**(2), 119–129, doi:10.1017/S14735504099990413.
- Wickramasinghe, C., Wallis, J. & Gibson, C.H. (2010a). *Proc. SPIE* **7819** (in press).
- Wickramasinghe, C., Wallis, M.K., Wallis, J., Gibson, C.H., Al-Mufti, S. & Nori, M. (2010b). *Proc. SPIE* **7819** (in press).
- Wickramasinghe, J.T. & Napier, W.M. (2008). *Mon. Not. Roy. Astr. Soc.* **387**, 153.
- Wickramasinghe, J.T., Wickramasinghe, N.C. & Napier, W.M. (2010c). *Comets and the Origin of Life*. World Scientific Publ., Singapore.
- Wickramasinghe, N.C., Wickramasinghe, J.T. & Mediavilla, E. (2004). *Astrophys. Space Sci.* **298**, 453.
- Witt, A. & Schild, R. (1988). *Astrophys. J.* **325**, 837.